

Discovery of an X-Ray Pulsar in the SMC: AX J0058–7203

Masahiro TSUJIMOTO, Kensuke IMANISHI, Jun YOKOGAWA, and Katsuji KOYAMA*
Department of Physics, Graduate School of Science, Kyoto University, Sakyo-ku, Kyoto, 606-8502
E-mail(MT): tsujimot@cr.scphys.kyoto-u.ac.jp

(Received 1999 August 18; accepted 1999 September 27)

Abstract

We report on the discovery and analysis of an X-ray pulsar, AX J0058–7203, in the Small Magellanic Cloud. This pulsar exhibits coherent pulsations at $P = 280.3$ s with a double-peak structure. The X-ray spectrum is well fitted with a simple power-law model of photon index $\Gamma \sim 0.7$. No significant change of the pulsation period over the observation was found. A comparison with ROSAT observations in the same field reveals that AX J0058–7203 is highly variable, and is most likely a Be star binary pulsar.

Key words: Magellanic Clouds — Pulsars: individual (AX J0058–7203) — X-rays: binaries

1. Introduction

X-ray binary pulsars (here XBPs) constitute a bright class of X-ray sources in the sky, and have been major objects for X-ray astronomy. Sporadic mass accretion from a companion star onto a spinning neutron star makes this class to be variable X-ray sources. X-ray binaries with a Be star companion (here Be-XBPs) are the most variable subclass; occasional outbursts may be caused by mass-ejection episodes of a companion Be star or by encounters with a dense stellar wind region along with a highly eccentric orbit of a neutron star. The average luminosity is generally lower than ordinal XBPs, and is typically in the range of 10^{34} – 10^{35} erg s $^{-1}$. This moderate luminosity together with a limited duty ratio of the outbursts has prevented us to perform a complete survey of this class with the conventional non-imaging instruments. The imaging instruments on-board the Einstein and ROSAT satellites greatly improved the detection threshold. Since XBPs (also Be-XBPs) generally exhibit a hard X-ray spectrum, contemporary hard X-ray satellites, ASCA (Advanced Satellite for Cosmology and Astrophysics), RXTE (Rossi X-ray Timing Explorer), and Beppo-SAX, further enhance the detection probability for this class of X-ray sources (XBPs and Be-XBPs).

In fact, multiple observations of the Small Magellanic Cloud (SMC) caused a rush of X-ray pulsar discoveries (Yokogawa et al. 1999). Among the known 16 X-ray pulsars in the SMC at present (Bildsten et al. 1997; Kahabka et al. 1999; Lamb et al. 1999; Macomb et al. 1999), 13 have been discovered within 1.5 years: from the end of 1997 to the middle of 1999. Most are considered to be Be-XBPs based on their transient nature and/or an op-

tical Be counterpart.

We report here on the discovery and analysis of AX J0058–7203, one of the newly discovered pulsars during the pulsar rush episode (Yokogawa, Koyama 1998). We also examine the flux variability using the archives of ASCA and ROSAT, and propose to classify this source as a Be star binary system in the SMC.

2. Observations

ASCA observed a SMC region centered at R.A.= $00^{\text{h}}59^{\text{m}}26^{\text{s}}.3$, Dec.= $-72^{\circ}10'12''.5$ (equinox 2000) on 1997 November 14 to 15, during the AO-6 cycle. The primary target of this observation was N66, one of SNRs in the SMC region. Details concerning the ASCA satellite as well as its instruments (GIS: Gas Imaging Spectrometer, SIS: Solid-state Imaging Spectrometer) and X-ray telescope (XRT) can be found in Tanaka et al. (1994), Ohashi et al. (1996), Makishima et al. (1996), Burke et al. (1991) and Serlemitsos et al. (1995). As is the nominal case, two GISs (GIS 2, 3) and SISs (SIS 0, 1) were operated in parallel.

AX J0058–7203 was in the field of view of the GISs and SISs at $\sim 13'$ off-axis positions. We excluded the data taken during the South Atlantic Anomaly or at an elevation angle less than 5° or the passage through a region where cut-off rigidity is lower than 6 GeV. In addition, we employed a rise-time discrimination technique to reduce particle events for the GIS data. After these filterings, the net exposure times were ~ 35 ks for GIS and ~ 31 ks for SIS.

3. Results and Analysis

* CREST, Japan Science and Technology Corporation (JST), 4-1-8 Honmachi, Kawaguchi, Saitama, 332-0012

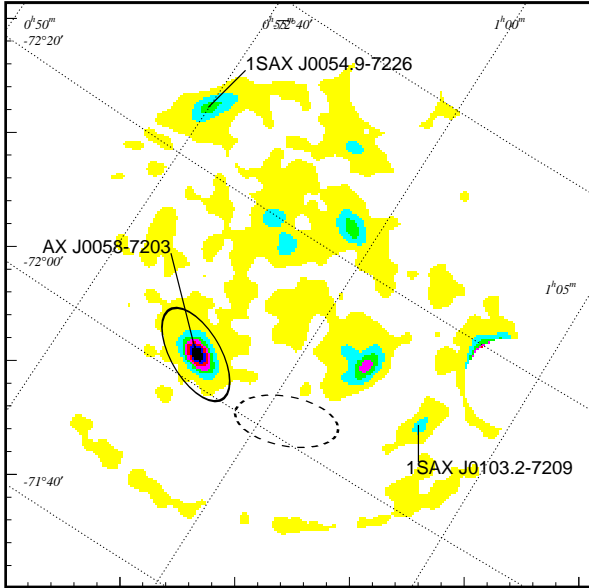


Fig. 1.. GIS hard-band image (2.0–7.0 keV): X-ray photons from the source are extracted from the region shown with the solid line. The background spectrum was taken from the dotted region, where the off-axis angle is almost the same as that of the source region. The calibration source regions of GIS 2 (at the top right) and GIS 3 (bottom right) are hollowed out.

3.1. X-Ray Image and Source Identification

A combined GIS image (GIS 2 + GIS 3) is shown in figure 1. The accurate position of this source was determined using two SIS images (SIS 0 and 1) to be R.A.= $00^{\text{h}}57^{\text{m}}53^{\text{s}}.3$, Dec.= $-72^{\circ}02'46''.5$ with an error circle of $\sim 40''$ in radius (Gotthelf 1996; ASCA News 4, 31), hence, we designate this source as AX J0058–7203. Two other X-ray pulsars are serendipitously located in the GIS field: 1SAX J0054.9–7226 with a pulsation period of 58.969 s (Santangelo et al. 1998) at the top left and 1SAX J0103.2–7209 with a pulsation period of 345.2 s (Israel et al. 1998) at the bottom right of figure 1. This demonstrates an extremely high density of X-ray pulsars of the central region of the SMC.

For source identification, we checked two comprehensive SMC source catalogs provided by Wang and Wu (1992) with Einstein observatory, and by Kahabka et al. (1999) with ROSAT observatory. Source No. 41 (SMC 0056.2–7219) in the former catalog and source No. 124 (RX J0057.8–7202) in the latter one are found to be located within the error circle of AX J0058–7203.

3.2. Temporal Analysis

The X-ray photons of AX J0058–7203 were extracted from the elliptical regions, as is indicated by the solid line in figure 1 for both the GIS and SIS data. We first confirmed that there was no flaring event nor any trend of flux variation during the observation. After a barycen-

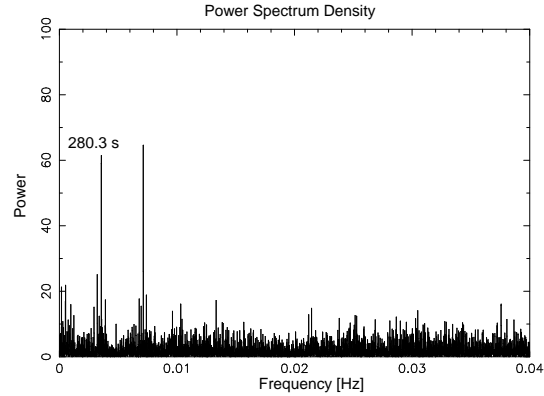


Fig. 2.. Power Spectrum Density of AX J0058–7203 for the GIS and SIS data in the 0.7–7.0 keV band. The fundamental pulsation together with the secondary harmonic can be clearly seen.

tric correction of the photon-arrival times, we conducted a Fast Fourier Transform (FFT), in order to search for any coherent periodicity. Figure 2 shows the power spectrum for the GIS data in the 0.7–7.0 keV band. We found two significant peaks at 3.6×10^{-3} Hz and 7.2×10^{-3} Hz. The chance probabilities to obtain these two peaks are estimated to be 9×10^{-10} and 1×10^{-11} , respectively. Since the frequency ratio between the two peaks is exactly double, we infer the lower frequency peak to be the fundamental period of $P = 280.3$ s and the higher to be the second harmonics.

We then employed a folding technique to the GIS and SIS data around a trial period of $P = 280.3$ s, and found the most likely period to be 280.4 ± 0.3 s. The folded pulse profile of 280.4 s period is given in figure 3. In the pulse profile, we can see two peaks, as was already expected from the power spectrum. Since the intensity of the main peak is about twice larger than that of the sub-peak, we conclude that 280.4 s is really the fundamental pulse period. The two-peak pulse profile does not change with the X-ray energy. The pulse fraction, defined as $(I_{\text{max}} - I_{\text{min}})/(I_{\text{max}} + I_{\text{min}})$, where I_{max} and I_{min} are the maximum and the minimum count rate including background photons, is 61% in the soft band (0.7–2.0 keV) and 48% in the hard band (2.0–7.0 keV). We also divided the full observation data into two data sets, the former half and the latter half, then separately applied the folding technic, but found no significant changes of the pulsation period over the observation period.

3.3. Spectral Analysis

Using the same source data as in the timing analysis (solid line in figure 1) and subtracting the background data in the dotted-line region in figure 1, we constructed the GIS and SIS X-ray spectra separately, showing the

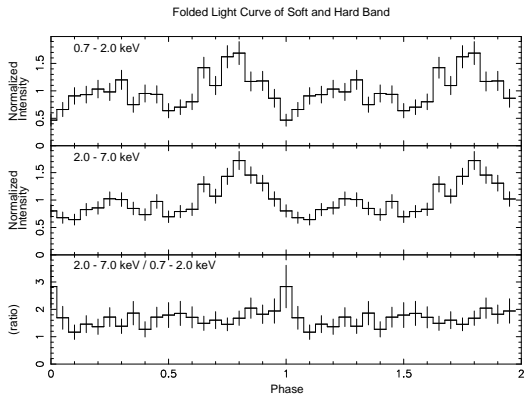


Fig. 3.. Pulse profiles in the two cycles for the soft band (0.7–2.0 keV: top panel), the hard band (2.0–7.0 keV: middle panel), and the intensity ratio of the two bands (bottom panel). The pulse profiles were constructed by using both the GIS and SIS data.

result in figure 4 with filled squares and circles, respectively. For our spectral analysis, both the GIS and SIS data in the energy band from 1.0 keV to 8.0 keV were binned so that each bin has at least 40 photons, and were fitted simultaneously.

For the continuum emission, we applied a power-law model with interstellar absorption, which is the “standard” model for X-ray binary pulsars (Nagase 1989), and obtained an acceptable fit. The best-fit parameters are given in table 1.

In figure 4, we can see a hint of excess at the energy of the $K\alpha$ line of He-like aluminum. To investigate the existence of this line emission, we fitted the spectrum with the absorbed power law with a Gaussian line centered at 1.59 keV ($K\alpha$ line of He-like aluminum). However, the significance level of this emission is less than $1\text{-}\sigma$ level. We also fitted the spectrum with the line-center variable, but no significant emission line (more than $1\text{-}\sigma$ level) was found.

The X-ray flux in the 0.7–10.0 keV band is calculated to be $\sim 3.0 \times 10^{-12}$ erg cm^{-2} s^{-1} based on the best-fit parameters, which indicates an absorption-corrected luminosity of $\sim 1.4 \times 10^{36}$ erg s^{-1} , assuming the distance to the SMC to be 60 kpc (Mathewson 1985).

4. Discussion

A long pulse period and a rather flat spectrum indicate this source to be an accretion-powered binary pulsar with a high-mass companion (Nagase 1989). Among high-mass binary pulsars with various types of optical companion, binary systems of an X-ray pulsar with a Be star share the transient nature which is exclusively found in this subclass (Stella et al. 1986).

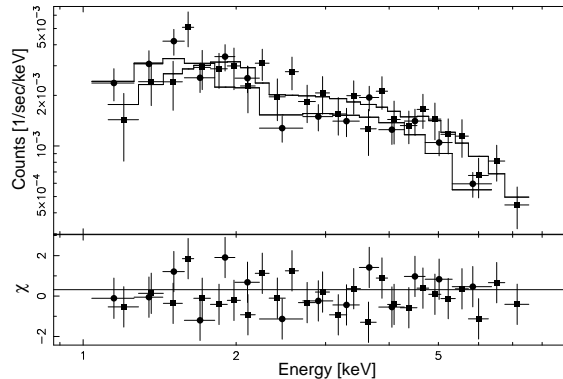


Fig. 4.. Upper panel: The GIS (filled squares) and SIS (filled circles) spectra of AX J0058–7203. The best-fit power law models of the simultaneous fitting are indicated by the solid lines. Lower panel: Residuals from the best-fit models.

Thus, information concerning the long-term flux variability of this source is critical to reveal its nature. We therefore used ROSAT and Einstein archival data which cover the region of AX J0058–7203 to search for its history of variability. The count rate, or upper limit, from this source are summarized in table 2 together with the ASCA result.

From table 2, we find that AX J0058–7203 shows a variation of more than 10 times in flux, which favors AX J0058–7203 to be a Be star binary pulsar. Due to limited data from this source the Be star interpretation still remains preliminary; hence, follow-up observations involving long-term pulsation monitoring and optical identification of a companion star are encouraged.

We thank all members of the ASCA team. This research has made use of data obtained through the High Energy Astrophysics Science Archive Research Center Online Service, provided by the NASA/Goddard Space Flight Center. J.Y. is supported by JSPS Research Fellowship for Young Scientists.

References

- Bildsten L., Chakrabarty D., Chiu J., Finger M.H., Koh D.T., Nelson R.W., Prince T.A., Rubin B.C. et al. 1997, *ApJS* 113, 367
- Burke B.E., Mountain R.W., Harrison D.C., Bautz M.W., Doly J.P., Ricker G.R., Danniels P.J. 1991, *IEEE Trans. ED-38*, 1069
- Israel G.L., Stella L., Campana S., Covino S., Ricci D., Oosterbroek T. 1998, *IAU Circ.* 6999
- Kahabka P., Pietsch W., Filipović M.D., Haberl F. 1999, *A&AS* 136, 81
- Lamb R.C., Prince T.A., Macomb D.J., Finger M.H. 1999, *IAU Circ.* 7081
- Macomb D.J., Finger M.H., Harmon B.A., Lamb R.C., Prince T.A. 1999, *ApJ* 518, L99
- Makishima K., Tashiro M., Ebisawa K., Ezawa H., Fukazawa Y., Gunji S., Hirayama M., Idesawa E. 1996, *PASJ* 48, 171
- Mathewson D.S. 1985, *Proc. Astron. Soc. Aust.* 6, 104
- Nagase F. 1989, *PASJ* 41, 1
- Ohashi T., Ebisawa K., Fukazawa Y., Hiyoshi K., Horii M., Ikebe Y., Ikeda, H., Inoue H. et al. 1996, *PASJ* 48, 157
- Santangelo A., Cusumano G., Israel G.L., Fiume D.D., Orlandini M., Frontera F., Parmar A.N., Marshall F.E. et al. 1998, *IAU Circ.* 6818
- Serlemitsos P.J., Jalota L., Soong Y., Kunieda H., Tawara Y., Tsusaka Y., Suzuki H., Sakima Y. et al. 1995, *PASJ* 47, 105
- Stella L., White N.E., Rosner R. 1986, *ApJ* 308, 669
- Tanaka Y., Inoue H., Holt S.S. 1994, *PASJ* 46, L37
- Wang Q., Wu X. 1992, *ApJS* 78, 391
- Yokogawa J., Imanishi K., Tsujimoto M., Nishiuchi M., Koyama K., Nagase F., Corbet R.H.D. 1999, *ApJ* submitted
- Yokogawa J., Koyama K. 1998, *IAU Circ.* 6853

Table 1. Best-fit parameters of the spectrum.

Detector	Photon index [†] Γ	Absorption [†] $N_{\text{H}}(10^{21} \text{ cm}^{-2})$	Reduced χ^2 (d.o.f.)
GIS	0.86 ± 0.23	4.8 ± 3.7	0.60 (26)
SIS	0.61 ± 0.22	2.6 ± 2.4	1.08 (14)
GIS+SIS	0.75 ± 0.19	3.6 ± 1.9	0.72 (40)

[†] Errors are for 90% confidence level.

Table 2. Flux history of AX J0058–7203.

Satellite	Detector	Date	Count rate [†] cnts s ⁻¹	Predicted X-ray flux ^{† ‡} erg cm ⁻² s ⁻¹
Einstein	IPC	1979/11/13	$(1.0 \pm 0.1) \times 10^{-4}$	$(5.4 \pm 0.5) \times 10^{-14}$
		1980/03/15	$< 1.9 \times 10^{-4}$	$< 1.0 \times 10^{-13}$
ROSAT	PSPC	1991/10/08	$(3.3 \pm 0.9) \times 10^{-3}$	$(6.4 \pm 1.8) \times 10^{-13}$
		1992/04/17	$< 1.7 \times 10^{-3}$	$< 3.3 \times 10^{-13}$
		1993/03/29	$< 1.2 \times 10^{-4}$	$< 2.4 \times 10^{-14}$
		1993/05/12	$(8.4 \pm 11.5) \times 10^{-4}$	$(1.6 \pm 2.2) \times 10^{-13}$
		1993/10/01	$(1.9 \pm 1.0) \times 10^{-3}$	$(3.7 \pm 2.0) \times 10^{-13}$
		1994/05/05	$(2.8 \pm 1.5) \times 10^{-3}$	$(5.4 \pm 2.9) \times 10^{-13}$
	HRI	1994/04/18	$< 5.7 \times 10^{-3}$	$< 3.1 \times 10^{-12}$
		1994/04/19	$< 1.7 \times 10^{-3}$	$< 9.2 \times 10^{-13}$
		1994/10/05	$< 4.9 \times 10^{-3}$	$< 2.6 \times 10^{-12}$
		1995/04/12	$(2.6 \pm 2.9) \times 10^{-3}$	$(1.4 \pm 1.6) \times 10^{-12}$
		1995/04/13	$< 8.5 \times 10^{-4}$	$< 4.6 \times 10^{-13}$
		1995/04/14	$< 1.0 \times 10^{-3}$	$< 5.4 \times 10^{-13}$
ASCA	GIS	1997/11/14	1.4×10^{-2}	3.2×10^{-12}

[†] Count rate with 1- σ error in a circle of 1' radius around the source position, after subtracting the background count rate taken in a neighboring off-source region. Upper limits for 1- σ significance level are given for observations in which the source was not detected.

[‡] X-ray flux 1- σ error in the 0.7–10.0 keV is simulated from the count rate by the `pimms` software, assuming no change from the ASCA spectrum. For those not detected, the upper limit is given. The ASCA result, together with the count rate, is also shown at the last row.